frontiers | Frontiers in Energy Research

ORIGINAL RESEARCH
published: 30 May 2022
doi: 10.3389/fenrg.2022.887006

Barocaloric Properties of Thermoplastic Elastomers

Naveen Weerasekera[1], *Kameswara Pavan Kumar Ajjarapu*[1], *Kavish Sudan*[1], *Gamini Sumanasekera*[2], *Kunal Kate*[1] *and Bikram Bhatia*[1]*

[1]Department of Mechanical Engineering, University of Louisville, Louisville, KY, United States, [2]Department of Physics and Astronomy, University of Louisville, Louisville, KY, United States

Solid-state refrigeration represents a promising alternative to vapor compression refrigeration systems which are inefficient, unreliable, and have a high global warming potential. However, several solid-state cooling technologies—including those relying on a temperature change induced by an applied electric field (electrocaloric effect), magnetic field (magnetocaloric effect), and uniaxial stress (elastocaloric effect)—have been investigated, but their efficiency and scalability remain a concern. Materials with a large barocaloric response—temperature/entropy change induced by hydrostatic pressure—hold a significant promise for solid-state cooling but remain comparatively less explored. These materials need to be inexpensive, compressible, and show a large barocaloric response around the temperature of interest. Soft materials have the potential to meet these requirements and enable the development of low-cost high-efficiency solid-state heat pumps. Here, we investigate the barocaloric performance of commercially available block copolymer thermoplastic elastomers. We characterized the mechanical, thermal, and barocaloric properties of these materials and evaluated their potential for solid-state refrigeration. We utilized rheometric measurements to evaluate the isothermal compressibility and normalized refrigerant capacity of the thermoplastic elastomers. In addition, we directly measured the pressure-induced temperature change of the test materials and compared them with their normalized refrigeration capacity. The measured isothermal compressibility was in the 0.1–0.4 GPa^{-1} range, while the normalized refrigeration capacity varied between 13.2 and 41.9 $kJ\,K^{-1}\,GPa^{-1}$ for a 100 MPa applied pressure and 65°C temperature span. The corresponding pressure-induced temperature change for an applied pressure of 434.1 MPa varied between 2.2 and 28°C. These results demonstrated the superior barocaloric properties of thermoplastic elastomers and their promise for next generation barocaloric solid-state refrigeration devices.

Keywords: thermoplastic elastomers, solid-state refrigeration, barocaloric effect, material characterization, rheology

OPEN ACCESS

Edited by:
Lin Zhao,
3M, United States

Reviewed by:
Angelo Maiorino,
University of Salerno, Italy
Jean Rodrigo Bocca,
State University of Maringá, Brazil

***Correspondence:**
Bikram Bhatia
bikram.bhatia@louisville.edu

Specialty section:
This article was submitted to Process and Energy Systems Engineering, a section of the journal Frontiers in Energy Research

Received: *01 March 2022*
Accepted: *13 April 2022*
Published: *30 May 2022*

Citation:
Weerasekera N, Ajjarapu KPK, Sudan K, Sumanasekera G, Kate K and Bhatia B (2022) Barocaloric Properties of Thermoplastic Elastomers. Front. Energy Res. 10:887006. doi: 10.3389/fenrg.2022.887006

INTRODUCTION

Air conditioning and refrigeration account for about a quarter of global total energy demand (US Energy Information Administration, 2021). These cooling needs are primarily met by vapor compression systems which are inefficient, unreliable, and have a high global warming potential (de Paula et al., 2020; Pol Lloveras and Josep-Lluís Tamarit, 2021). Solid-state

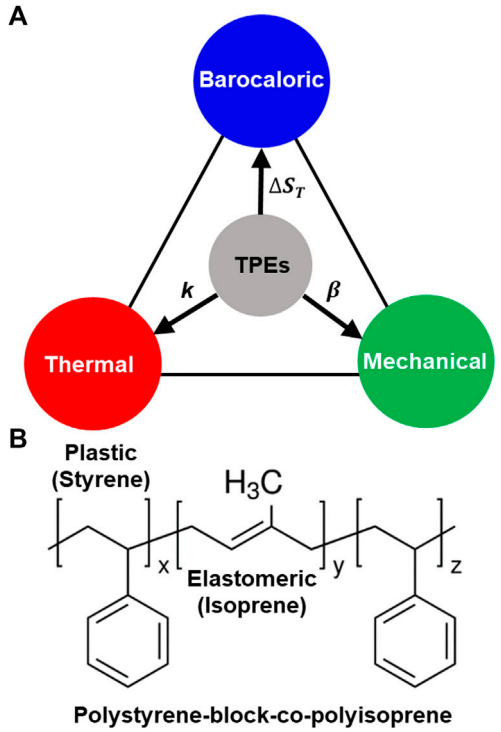

FIGURE 1 | Thermoplastic elastomers (TPEs) as promising barocaloric materials. **(A)** Different material properties relevant for solid-state refrigeration based on the barocaloric effect. These include compressibility (β), thermal conductivity (k), and barocaloric entropy change (ΔS_T). **(B)** TPEs comprise a plastic and an elastomeric component—shown here for a typical block copolymer (polystyrene-co-block-polyisoprene).

refrigeration (SSR)—utilizing the caloric response of materials subjected to external stimuli—provides a promising alternative to the vapor compression technology and has consequently received significant attention over the last three decades (Greco et al., 2019). Recent studies have investigated a wide variety of materials for SSR when subjected to an external electric field (based on the electrocaloric effect), magnetic field (based on the magnetocaloric effect), uniaxial stress (based on the elastocaloric effect), or hydrostatic pressure (based on the barocaloric effect) (Kitanovski et al., 2015). However, solid-state cooling technologies are not yet competitive with vapor compression systems and require investigation of different material systems and operational modalities (Kitanovski et al., 2015; Qian et al., 2016).

Solid-state cooling based on the barocaloric (BC) effect is among the least studied caloric technologies but has received a significant interest in the last few years due to the large barocaloric responses reported in several material classes (Aprea C. et al., 2019; C.; Aprea et al., 2018a; Aprea G. et al., 2019; Aznar et al., 2020; Garcia-Ben et al., 2021; Greco et al., 2019; Miliante et al., 2020; Min et al., 2020; Moya and Mathur, 2020; Lloveras and Tamarit, 2021). The barocaloric response of a material subjected to hydrostatic pressure is characterized by the resulting isothermal entropy change (ΔS_T) or, equivalently, the adiabatic temperature change (ΔT_s). Another key BC performance metric that connects the material BC response with its useful heat pumping capacity between a specified temperature range (ΔT_{h-c}) is the normalized refrigerant capacity (NRC) (Usuda et al., 2019). The NRC is normalized by the applied pressure (Δp) and, therefore, factors in the challenge of achieving high pressures—a key bottleneck for BC cooling. These BC metrics, however, only represent the thermodynamic performance and do not account for the effectiveness of mechanical force transmission and heat conduction which are also critical for SSR devices. Previous studies have shown that the isothermal volumetric compressibility (β) of a material is directly correlated with its BC performance (Li et al., 2019). In addition, the heat transfer to/from the hot/cold reservoir is dependent on its thermal conductivity (k) and specific heat capacity (c_p) (Aprea et al., 2020; C.; Aprea G. et al., 2019; Maiorino et al., 2019). The performance of a BC SSR device is, thus, dependent on the material barocaloric, mechanical, and thermal properties (**Figure 1A**).

The BC effect has been demonstrated and investigated in a wide variety of materials (Boldrin, 2021) including soft materials, organic–inorganic salts, perovskites, and magnetic shape memory alloys (Mañosa et al., 2010; Patel et al., 2016; Li et al., 2019; Miliante et al., 2020). Despite their typically low thermal conductivity, soft materials are particularly attractive due to their large BC response, high compressibility, and low cost. One class of soft materials that has received significant attention is plastic crystals whose first-order phase transitions near room temperature lead to colossal ΔS_T values > 500 J kg^{-1} K^{-1} ($\Delta p \approx 500$ MPa) (Li et al., 2019, 2020; Lloveras and Tamarit, 2021). In addition to plastic crystals, a wide range of polymers have shown promising BC properties. Patel et al. (2016) observed a BC $\Delta T_s \approx 6$°C at room temperature ($\Delta p \approx 200$ MPa) in polyvinylidene difluoride–based polymers. Furthermore, the BC effect was investigated in several elastomers. These included nitrile butadiene rubber which achieved a BC $\Delta S_T \approx 60$ J kg^{-1} K^{-1} and $\Delta T_s \approx 15$°C ($\Delta p = 390$ MPa) near room temperature (Usuda et al., 2019). The range of the NRC reported for ΔT_{h-c} values of 5–75°C was 1–13 kJ K^{-1} GPa^{-1}. A higher ΔS_T up to 250 J kg^{-1} K^{-1} and ΔT_s up to 25°C were measured for natural rubber, albeit at a higher applied pressure ($\Delta p \approx 500$ MPa) (Miliante et al., 2020). Comparable BC properties were also demonstrated in polyurethane rubber (Bocca et al., 2021)—achieving NRC ≈11 kJ kg^{-1} GPa^{-1} (Δp = 174 MPa)—and PDMS rubber (Carvalho et al., 2018)—achieving NRC ≈9 kJ kg^{-1} GPa^{-1} (Δp = 193 MPa)—for ΔT_{h-c} = 25°C. The BC properties of these materials were evaluated by pressure-dependent differential scanning calorimetry, indirect methods based on Maxwell's relations, or quasi-adiabatic direct measurements (Li et al., 2019; Lloveras et al., 2019; Usuda et al., 2019; Bocca et al., 2021). Although impressive barocaloric entropy and temperature changes have been observed in different classes of materials, the performance is still not sufficient to compete with conventional refrigeration technologies due to challenges associated with the thermal transport, reliability and cost. Thus, it is crucial to search and

TABLE 1 | List of materials studied. Thermoplastic elastomers (TPEs) tested, their classification, composition and common name, and melting temperature at ambient pressure and temperature obtained from DSC measurements.

TPE type	Thermoplastic elastomer	Thermoplastic component	Elastomeric component	Commercial/ common name	Melting temperature
Styrenic block copolymer (SES)	Polystyrene-co-block-polyisoprene	Polystyrene	Polyisoprene	SBPI	322.1°C
	Polystyrene-block-polybutadiene	Polystyrene	Polybutadiene	SBPB	359°C
Thermoplastic copolyester (TPC)	Polyester-block-polycaprolactane	Polyester	Polyether	Hytrel™	131.1°C
	Polyester-block-polyether	Polybutylene tetraphthalate	Polyester	PIBIFLEX™	224°C
Thermoplastic polyurethane (TPU)	Polycaprolactane-block-polyurethane	Polycaprolactane	Polyurethane	ESTANE™	218°C
	Polyether-block-polyurethane	Polyether	Polyurethane	PELLETHANE™	205.2°C
Thermoplastic polyethylene (TPE)	Poly (ethylene-co-vinyl acetate)	Polyethylene	Co-vinyl acetate	ELVAX™	86.8°C
	Poly (ethylene-co-vinyl alcohol)	Polyethylene	Co-vinyl alcohol	EVCA	189°C
Thermoplastic polyamide (TPA)	Polyether-block-polyamide	Polyamide	Polyether	PEBAX™	162°C
	Glass-reinforced polyamide	Polyamide	-	Zytel™	251.5°C

investigate new materials that have good barocaloric performance, high thermal conductivity, and mechanical durability capable of undergoing repeated compression cycles over their operating lifetime and are available at low cost.

Although several polymers have demonstrated encouraging barocaloric properties, a class of soft materials that has not yet been investigated is thermoplastic elastomers (TPEs). TPEs are polymers with two distinct building blocks—a thermoplastic (hard) part comprising a glassy/semicrystalline material and an elastomeric (soft) part comprising a pure amorphous material (**Figure 1B**) (Roth et al., 2020). The soft elastomeric component confers high compressibility and a high BC response due to the large pressure-induced conformational changes in the polymer, while the semicrystalline component increases the phonon density of states, enhancing the thermal transport (dos Santos et al., 2008; Xu et al., 2020). Thus, TPEs represent a promising class of materials that can simultaneously achieve high isothermal volumetric compressibility (β), high isothermal barocaloric entropy change (ΔS_T), and high thermal conductivity (k) (Kıroğlu and Kızılcan, 2021). In addition, TPEs have relatively low melting points (<300°C) and can be easily fashioned into different shapes and sizes using manufacturing processes such as injection molding and extrusion-based additive manufacturing (Heckele and Schomburg, 2004) (Raasch et al., 2015). Furthermore, a wide range of TPEs with varying thermomechanical properties are commercially available at low cost. This study investigates the barocaloric properties of TPEs as potential BC refrigerant material for next-generation SSR systems.

In this work, we characterized the barocaloric and related properties of commercially available TPEs. The pressure–volume–temperature (pvT) relationships of the materials are obtained in the 35–100°C temperature range and at pressures <100 MPa using a rheometer. The pvT data are used to evaluate the isothermal compressibility (β), the normalized refrigerant capacity (NRC), and related BC properties. We also measured the thermal conductivity of the TPEs at their melting temperature using the same rheological apparatus. In addition to the rheometric measurements, we also used a custom-fabricated experimental setup to directly measure the quasi-adiabatic temperature change of the TPEs when subjected to hydrostatic pressure near room temperature. The quasi-adiabatic measurement, based on methods reported in the literature (Usuda et al., 2019), enables direct determination of the barocaloric temperature change and provides qualitative validation of the rheological measurements. Finally, we compared the barocaloric, mechanical, and thermal properties of the different TPEs and identified the most promising candidates for solid-state heat pumping.

MATERIALS

We investigated barocaloric and related properties of block copolymer TPEs near room temperature (20–100°C). Block copolymers are widely accessible at a low cost from numerous manufacturers. **Table 1** lists the TPEs studied and their key components. For this study, we identified commercially important TPEs based on styrenic block copolymers, thermoplastic copolyesters, thermoplastic polyurethanes, ethylene-based copolymers, and thermoplastic polyamides (Holden, 1987). In this work, we tested nine TPEs and one pure thermoplastic material (ZYTEL) chosen based on their commercial availability. The material selection also ensured the TPEs were usable at room temperature, that is, the glass transition temperature of the elastomeric part was lower than room temperature, and the glass transition temperature of the thermoplastic part was sufficiently higher than room temperature. All materials obtained were in the form of millimeter-scale pellets (additional details regarding the material suppliers are provided in **Supplementary Section S1**).

METHODS

We performed material characterization to obtain mechanical, thermal and BC properties by rheometry, differential scanning calorimetry (DSC), and quasi-adiabatic direct measurement techniques. Atmospheric pressure DSC measurements were initially used to characterize the melting temperatures of

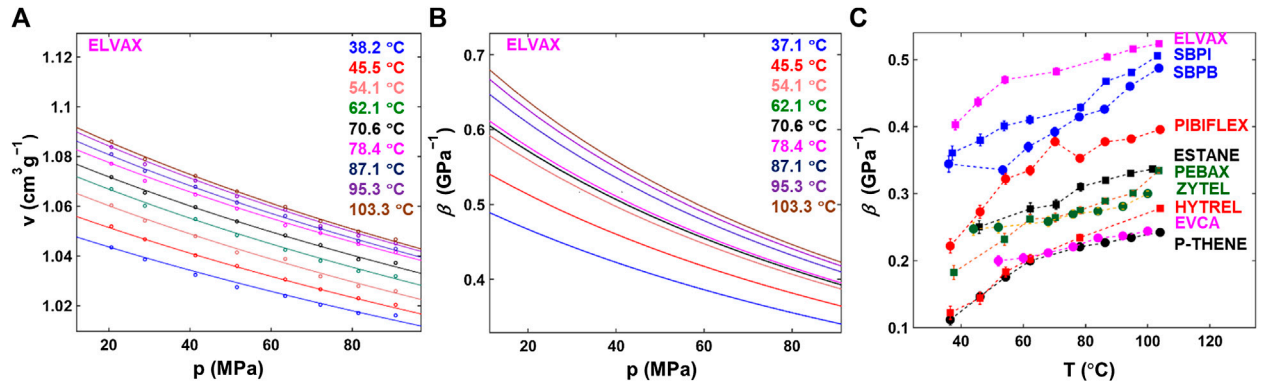

FIGURE 2 | Mechanical property measurement. **(A)** *pvT* isotherms (symbols) fitted with the Tait equation of state (solid lines) for a representative material (ELVAX). **(B)** Temperature-dependent isothermal compressibility calculated using the isotherms plotted as a function of pressure for ELVAX. **(C)** Isothermal compressibility of all materials as a function of temperature at 50 MPa pressure.

different materials and confirm their suitability for the study. We also used the DSC data to identify other relevant (solid–solid) phase transitions near room temperature and evaluate the specific heat capacity of the material (**Supplementary Section S2**). In addition, we performed direct barocaloric characterization by measuring the temperature change induced in each material when subjected to hydrostatic pressure. These quasi-adiabatic measurements were performed near ambient temperature (20°C) using a custom-fabricated test setup described in **Supplementary Section S7**. These direct and indirect measurements allowed us to investigate the barocaloric properties of TPEs and evaluate their potential for solid-state refrigeration.

Isothermal Compressibility

To determine the isothermal compressibility (β) of each material, we obtained pressure–volume–temperature (pvT) data using a capillary rheometer in the 10–90 MPa pressure range. We acquired pvT isotherms varying the pressure using a piston setup while monitoring the displacement to calculate the material volume and ensuring it is maintained at a constant temperature. The material temperature is monitored using three thermocouples surrounding the pvT capillary and a thermocouple attached to the capillary die. The complete description of the pvT testing process is presented in **Supplementary Section S3**.

Figure 2A presents pvT isotherms for a representative material (ELVAX) at different temperatures. Each isotherm—showing a decreasing specific volume with increasing pressure and decreasing temperature—is fitted with the Tait equation of state (**Supplementary Section S3**) (Pottiger et al., 1994). The volumetric compressibility at constant temperature (β) is obtained by evaluating the gradients of the isotherms (Janssen et al., 1995).

$$\beta = \frac{1}{v_0}\left(\frac{\partial v}{\partial p}\right)_T, \tag{1}$$

where v_0 is the initial specific volume at atmospheric pressure. **Figure 2B** shows β as a function of pressure at different temperatures for ELVAX (data for other materials are included in **Supplementary Section S4**). The results indicate that the compressibility decreases at higher pressures but increases at elevated temperatures. β values for all materials are shown as a function of temperature at a pressure of 50 MPa in **Figure 2C**. We observed β increases with increasing temperature at constant pressure due to softening of the material as it approaches its melting temperature—consistent with prior results for thermoplastic compounds (Roth et al., 2020). The overall range of compressibility values obtained (0.1–0.6 GPa^{-1}, measurement uncertainty <0.3%) is comparable to that for elastomers and plastic crystals reported in the literature (Li et al., 2019). However, the values for TPEs are slightly lower than some highly compressible elastomers such as rubber due to the increase in hardness with the addition of the thermoplastic component (Fazli and Rodrigue, 2020). Overall, the highest β values in the 0.4–0.53 GPa^{-1} range are observed for ELVAX in the measurement temperature span of 35–100°C.

Thermal Conductivity

The thermal conductivity (k) of each polymer is measured at its respective melting temperature *via* the transient line source (TLS) method implemented using the rheometer. The TLS measurement used a thermal conductivity probe with an embedded linear heat source and thermocouple to heat and measure the transient temperature of a cylindrical material specimen. The temperature rise of the sample as a function of time is fitted using the transient heat conduction equation to calculate the material thermal conductivity. **Figure 3A** shows the raw data used to calculate the thermal conductivity for one of the materials tested (ELVAX). Additional information regarding the thermal conductivity measurement and raw data for other materials are provided in **Supplementary Section S5**. In addition to thermal conductivity, we also measured the temperature-dependent specific heat capacity of the materials using DSC (**Figure 3B**; **Supplementary Section S2**).

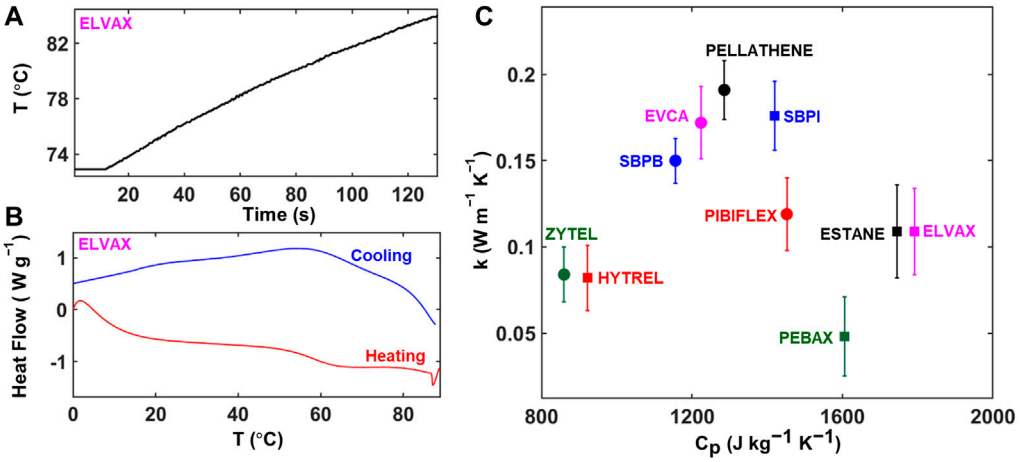

FIGURE 3 | Thermal property measurement. **(A)** Transient temperature profile from the thermal conductivity measurement for a representative material (ELVAX). **(B)** DSC endo- and exotherms used for specific heat capacity calculation shown for ELVAX. **(C)** Plot showing the melt thermal conductivity and specific heat capacity at 35°C for the TPEs tested.

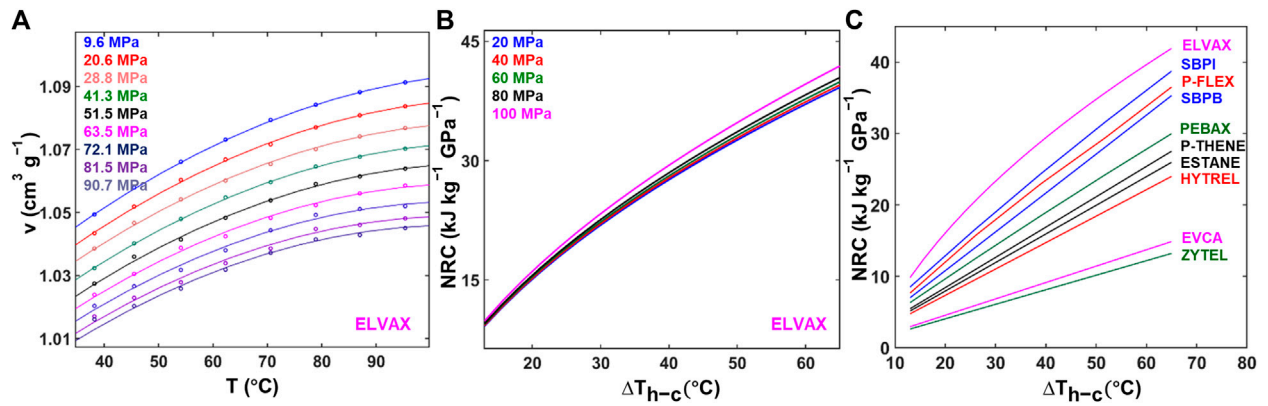

FIGURE 4 | Barocaloric property measurement. **(A)** *pvT* isobars shown for a representative material (ELVAX) (solid lines represent the Tait equation fits for each isobar). **(B)** Normalized refrigerant capacity (NRC) calculated for a cold reservoir temperature of 35°C and varying temperature spans (ΔT_{h-c}) and pressures shown for ELVAX. **(C)** NRC as a function of ΔT_{h-c} for all materials (measurement uncertainty <0.3%) evaluated for Δp = 100 MPa.

Figure 3C shows the measured thermal conductivity and specific heat capacity for all materials tested to compare their heat transfer properties. As would be expected from thermally insulating polymers, the thermal conductivities of the materials tested are relatively low (<0.2 W m^{-1} K^{-1}; measurement uncertainty <0.05 W m^{-1} K^{-1}). The thermal conductivities are, however, comparable to those of typical elastomers (e.g., silicone rubber ~0.18 W m^{-1} K^{-1}) (Kashi et al., 2018; Gschwandl et al., 2019; Mirizzi et al., 2021); the addition of thermoplastics did not result in a significant increase in k for the studied TPEs. However, consistent with our understanding of the TPE structure, we observed a higher thermal conductivity for the pure thermoplastic (ZYTEL) than its corresponding TPE (PEBAX) which additionally includes an elastomeric component. The specific heat capacities of the TPEs studied varied from 821 J kg^{-1} K^{-1} (ZYTEL) to 1,792 J kg^{-1} K^{-1} (ELVAX), with c_p for most materials around 1,300 J kg^{-1} K^{-1}. For reference, the specific heat capacity of a pure elastomer (silicone rubber) is similar ~1,300 J kg^{-1} K^{-1} (Kashi et al., 2018).

Barocaloric Properties

Maxwell's relations are used to calculate the BC isothermal entropy change (ΔS_T) from the measurement of volumetric thermal expansion behavior as a function of temperature for different pressures. *pvT* isobaric measurements are performed maintaining a constant pressure on the material sample while ramping the temperature at a constant rate maintaining local

thermal equilibrium (Wang et al., 2019). **Figure 4A** shows pvT isobars for ELVAX in the 35–100°C temperature range for different pressures with the corresponding Tait equation fits (isobars for other materials are included in **Supplementary Section S3**). The isothermal entropy change is then calculated based on the gradients of the relative specific volume change over the pressure range of interest (Usuda et al., 2019),

$$\Delta S_T = -v_0 \int_{p_1}^{p_2} \left(\frac{\partial\left(\frac{\Delta v}{v_0}\right)}{\partial T} \right)_p dp, \tag{2}$$

where Δv is the specific volume change from its initial value v_0 due to a change in the temperature at a specific pressure. The overall ΔS_T is evaluated as the pressure increases/decreases from p_1 to p_2 as the material is hydrostatically compressed/expanded. To estimate the potential of the BC material, we then determined its normalized refrigerant capacity for SSR operation between a hot thermal reservoir (at temperature T_h) and cold thermal reservoir (at temperature T_c) (Usuda et al., 2019).

$$NRC\left(\Delta T_{h-c}, \Delta p\right) = \left| \frac{1}{\Delta p} \int_{T_c}^{T_h} \Delta S_T\left(T, \Delta p\right) dT \right|. \tag{3}$$

This NRC value is dependent on the temperature range of operation $\Delta T_{h-c} = T_h - T_c$ and is normalized by the applied pressure Δp. Additional details regarding NRC calculation are provided in **Supplementary Section S6**.

Figure 4B shows the NRC of ELVAX as a function of ΔT_{h-c} calculated from pvT isobars for T_c = 35°C for five Δp values up to 100 MPa. The NRC increases at higher ΔT_{h-c} since more heat is pumped for a larger temperature span. The nature of the dependence of NRC on ΔT_{h-c} and Δp is, however, dependent on the pvT relationship of the material. A slightly higher NRC is observed for a higher Δp, particularly at large ΔT_{h-c}, because of the non-linear increase in ΔS_T due to the solid-state second-order phase transition in ELVAX, which can be attributed to the crystalline-to-amorphous transition (beta transition) within the TPE (Brogly et al., 1998). This solid-state phase transition is also observed in the DSC thermogram in the ~0–70°C temperature span (**Figure 3B**). A similar broad phase transition was observed in previous studies on related copolymers with 18% vinyl acetate content (Wang and Deng, 2019). **Figure 4C** shows the NRC values of all materials as a function of ΔT_{h-c} for a Δp of 100 MPa. Unlike ELVAX, the NRC for all other materials varies nearly linearly with ΔT_{h-c} since they do not undergo any phase transformation. Overall, the TPE NRC values are comparable to those for pure elastomers reported earlier (≈10 kJ kg^{-1} GPa^{-1} for ΔT_{h-c} = 25°C (Carvalho et al., 2018; Usuda et al., 2019), but higher values are measured for ELVAX while lower values are measured for the less compressible EVCA and the thermoplastic ZYTEL.

RESULTS AND DISCUSSION

The performance of solid-state materials as refrigerants for SSR is dependent on their barocaloric, mechanical, and thermal properties. **Figure 5** summarizes the barocaloric property measurements—showing the normalized refrigerant capacity (at T_c = 35°C, T_h = 100°C, and Δp = 100 MPa) as a function of isothermal compressibility (at 35°C and 50 MPa) and the melt thermal conductivity of the materials tested. Comparing NRC and β (**Figure 5A**), it is evident that high compressibility is generally correlated with a high NRC, as shown by the measurements for ELVAX, SBPI and SBPB. This relationship between the NRC and β is primarily due to the larger hydrostatic strain developed for the same applied pressure in materials with high compressibility. However, the TPE structure and composition also influences these properties, as shown by the lower NRC measured for the purely thermoplastic ZYTEL. Unlike the correlation between mechanical and barocaloric properties, the thermal conductivity does not appear to have an impact on the NRC (**Figure 5B**). This apparent disconnect between k and NRC is because the rheological-based barocaloric measurements were performed under quasi-equilibrium conditions which were not influenced by the thermal transport. However, heat transfer plays a crucial role in the design and operation of a SSR device. Thus, higher thermal conductivity materials are preferable. Overall, these results indicate TPEs such as ELVAX, SBPI and SBPB that are highly compressible, reasonably thermally conducting, and have a high barocaloric refrigerant capacity are good candidate materials for SSR.

In addition to rheometric measurements, we also used a custom-fabricated quasi-adiabatic test setup similar to that reported in the literature (Bom et al., 2018) to directly measure the pressure-induced temperature change of all materials. **Figures 6A,B** show the test rig used to measure the BC response of the polymers around ambient temperature (~20°C). The setup comprises a rigid enclosure that holds the BC material which is subjected to compression-expansion cycles using a hydraulic press-driven piston. **Figure 6C** shows the results of a typical quasi-adiabatic BC temperature change measurement for ELVAX at a maximum pressure of 434.1 MPa. A detailed description of direct BC measurement setup, experimental procedure and raw data are included in **Supplementary Section S7**.

Figure 6D shows the measured quasi-adiabatic temperature change (ΔT_{q-ad}) as a function of maximum applied pressure for all materials tested. ΔT_{q-ad} increases monotonically with increasing Δp corresponding to a higher barocaloric entropy change at greater pressures. The conformational change-driven entropy increase/decrease within the TPEs is reversible—shown by the consistent results obtained for multiple cycles—and does not appear to saturate in the range of pressures investigated. Overall, we measured the highest ΔT_{q-ad} value of 28°C (±0.75% measurement uncertainty) for a Δp of 434.1 MPa for ELVAX, while the lowest value was reported for ZYTEL.

The data from the quasi-adiabatic approach can be compared with the results obtained using rheometric measurements. **Figure 7** shows the barocaloric NRC (for Δp = 100 MPa and ΔT_{h-c} = 65°C) evaluated using pvT measurements and the directly measured ΔT_{q-ad} (for Δp = 434.1 MPa) for all materials. The data points on the NRC versus ΔT_{q-ad} plot fall

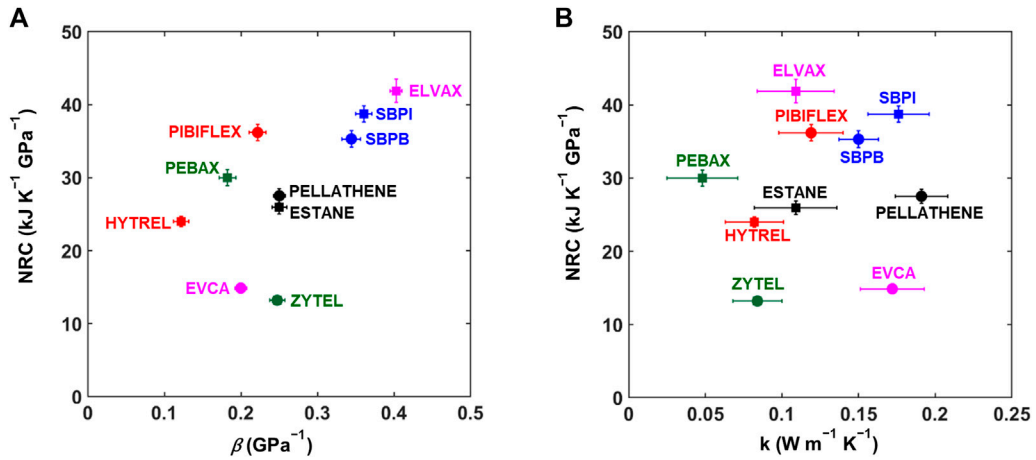

FIGURE 5 | Mechanical, thermal, and barocaloric properties. **(A)** Normalized refrigerant capacity (NRC, shown for Δp = 100 MPa and ΔT_{h-c} = 65°C) and isothermal compressibility (β at 35°C and 50 MPa) of the TPEs tested. **(B)** NRC and melt thermal conductivity (k) of the materials characterized.

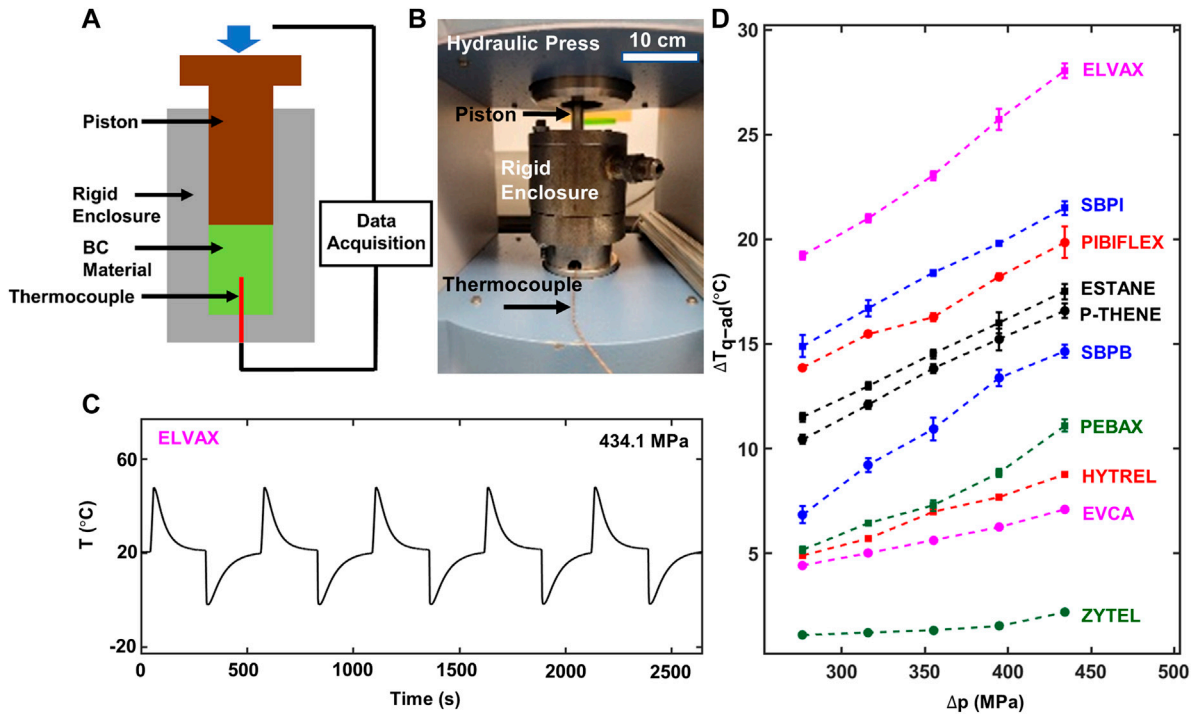

FIGURE 6 | Direct barocaloric temperature change measurement. **(A)** Schematic representation and **(B)** photograph of the custom-fabricated setup for the direct measurement of the pressure-induced temperature change. **(C)** Measured temperature of a representative material (ELVAX) subjected to five pressure (Δp = 434.1 MPa) applications and release cycles. **(D)** Measured temperature rise as a function of applied pressure (Δp) for the materials tested around room temperature.

approximately on a diagonal, indicating a direct correlation and agreement between the rheometric and direct measurements. Although NRC and ΔT_{q-ad} were obtained for different pressure ranges due to the constraints imposed by our equipment, the results indicated we can reasonably extrapolate the results and make qualitative comparisons. Furthermore, the NRC is a thermodynamic metric evaluated based on measurements under near-equilibrium conditions, while ΔT_{q-ad} is measured directly and depends on thermal transport (and corresponding thermal properties, k and c_p). Nevertheless, the measured NRC and ΔT_{q-ad} values are qualitatively consistent and can be used to identify promising barocaloric materials.

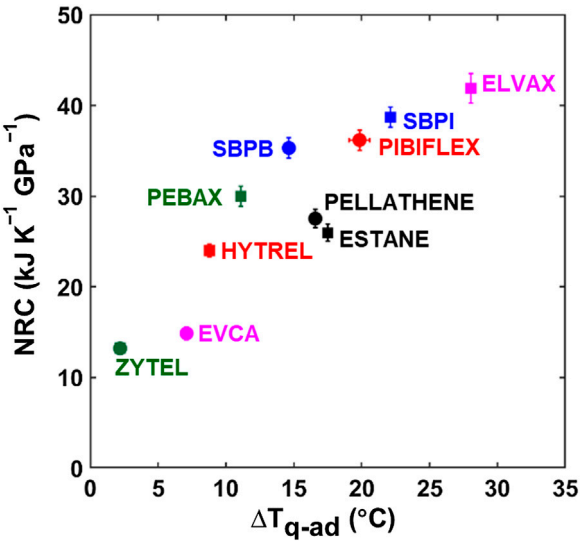

FIGURE 7 | Direct versus indirect barocaloric measurement. Comparison of the normalized refrigeration capacity (NRC, for Δp = 100 MPa and ΔT_{h-c} = 65°C) evaluated based on *pvT* measurements and the quasi-adiabatic temperature change (ΔT_{q-ad}) measured (Δp = 434.1 MPa) using the custom test rig for the materials tested.

The performance of barocaloric materials is dependent upon their compressibility, thermal conductivity and heat capacity, and BC entropy change. Among the materials studied in this study, the highest NRC and ΔT_{q-ad} were measured for ELVAX—a TPE with polyethylene as the thermoplastic component and co-vinyl acetate as the elastomeric component. Its superior barocaloric performance can be attributed to its solid–solid phase transition in the 0–70°C temperature range and high compressibility. These properties enabled ELVAX to demonstrate cooling to temperatures less than 0°C during the quasi-adiabatic measurements (applied pressure: 434.1 MPa). TPEs such as SBPI and SBPB—with reasonably high compressibility and barocaloric NRC, and thermal conductivity higher than ELVAX—also hold a promise for BC SSR. Meanwhile, the thermoplastic ZYTEL exhibited the worst barocaloric properties among the materials tested due to the absence of an elastomeric part in its structure. We also noticed that some relatively hard materials (low β), such as HYTREL, also showed decent BC properties likely due to the elastomeric contribution. These results indicate dependence of barocaloric properties on the type and quantity of the elastomeric component in a TPE. Although the addition of the thermoplastic component can improve the thermal conductivity of the TPE, it usually comes at a cost of lower ΔS_T and β. Several of these observations are, however, based on a qualitative understanding of our results that considered a wide range of TPE materials. Future work that systematically investigates the effect of different thermoplastic/elastomeric components and their relative amounts could provide further insight into the properties of TPEs and their potential as barocaloric refrigerant materials.

Another key metric relevant for the performance of a refrigerator is the coefficient of performance (COP). To predict the performance of the tested barocaloric materials as

TABLE 2 | Comparison of the current work with previous studies on barocaloric properties of soft materials.

Material name	Material type	Adiabatic/quasi-adiabatic ΔT (K) (Δp (MPa))	Material COP (Δp (MPa))	References
Neopentyl glycol (NPG)	Plastic crystal	$12^{q\text{-}ad}$ (100)	-	(Li et al., 2019; Lloveras et al., 2019; Boldrin, 2021)
Pentaglycerin (PG)	Plastic crystal	$10^{q\text{-}ad}$ (100)	-	(Li et al., 2019; Aznar et al., 2020; Boldrin, 2021)
Neopentyl alcohol (NPA)	Plastic crystal	~12.5 (100)	-	(Li et al., 2019; Aznar et al., 2020; Boldrin, 2021)
2-Amino-2-(hydroxymethyl)propane-1,3-diol (TRIS)	Plastic crystal	~4 (100)	-	Aznar et al. (2020)
2-Amino-2-methyl-1,3-propanediol (AMP)	Plastic crystal	~7 (600)	-	Aznar et al. (2020)
PVDF-TrFE-CTFE	Polymer	$\sim 10^{q\text{-}ad}$ (80)	-	(Patel et al., 2016; Aprea et al., 2018)
Polydimethylsiloxane (PDMS)	Elastomer	$28.5^{q\text{-}ad}$ (390)	9 (87)	Carvalho et al. (2018)
Waste tire rubber	Elastomer	$21^{q\text{-}ad}$ (390)	-	Bom et al. (2020)
Natural rubber	Elastomer	$25^{q\text{-}ad}$ (390)	-	Bom et al. (2018)
Nitrile butadiene rubber	Elastomer	$16.4^{q\text{-}ad}$ (390)	~4 (173)	Usuda et al. (2019)
Polyurethane	Elastomer	$15^{q\text{-}ad}$ (218)	-	Bocca et al. (2021)
SBPI	TPE	$21.5^{q\text{-}ad}$ (434)	11.5 (100)	Current work
SBPB	TPE	$14.64^{q\text{-}ad}$ (434)	8.9 (100)	Current work
Hytrel	TPE	$8.78^{q\text{-}ad}$ (434)	8.4 (100)	Current work
PIBIFLEX	TPE	$19.84^{q\text{-}ad}$ (434)	10.8 (100)	Current work
ESTANE	TPE	$17.5^{q\text{-}ad}$ (434)	9.1 (100)	Current work
PELLETHANE	TPE	$16.58^{q\text{-}ad}$ (434)	8.3 (100)	Current work
ELVAX	TPE	$28.04^{q\text{-}ad}$ (434)	16.5 (100)	Current work
EVCA	TPE	$7.1^{q\text{-}ad}$ (434)	2.5 (100)	Current work
PEBAX	TPE	$11.1^{q\text{-}ad}$ (434)	8.3 (100)	Current work
Zytel	Thermoplastic	$2.2^{q\text{-}ad}$ (434)	2.4 (100)	Current work

The table shows the studied material, material type, adiabatic/quasi-adiabatic (q-ad) temperature change (ΔT) resulting from the applied pressure change (Δp), and the material coefficient of performance (COP) calculated for a representative Δp.

solid-state refrigerants, we evaluated the material COP using the methods described in the literature (Carvalho et al., 2018; Schmidt et al., 2016; Usuda et al., 2019). Details are given in **Supplementary Section S8**. **Table 2** lists the predicted COP values of the tested materials calculated for a working temperature of 35°C and compared with the barocaloric performance of other soft materials reported in the literature. The COP values of the TPEs studied in this work are comparable to those reported for pure elastomeric compounds (Carvalho et al., 2018; Usuda et al., 2019). The COP values are also consistent with the NRC values described earlier, demonstrating ELVAX, SBPI and SBPB as promising barocaloric materials for refrigeration.

CONCLUSION

This study reports a large barocaloric response in TPEs at relatively low applied pressures ≲100 MPa. We identified and experimentally measured mechanical, thermal and BC properties that are relevant for SSR. Mechanical characterization relied upon the volumetric compressibility, while thermal characterization focused on the thermal conductivity of the materials. The BC properties of the materials were quantified by their NRC evaluated using rheometric measurements and directly measured quasi-adiabatic temperature change. The rheometric pvT measurements of the soft materials facilitated the calculation of barocaloric ΔS_T and NRC using Maxwell's relations, which were compared with direct BC temperature change measurements and realized using a custom setup. Overall, we characterized ten commercially available block copolymers near room temperature. We demonstrated NRC values as high as 41.9 J kg^{-1} K^{-1} for a hydrostatic pressure of 100 MPa and 65°C temperature span and a maximum ΔT_{q-ad} of 28°C for an applied pressure of 434.1 MPa. These NRC and ΔT_{q-ad} values are comparable to the highest values reported for elastomers, indicating the promise of TPEs as BC materials. Of the ten materials tested, we identified three commercially available TPEs—ELVAX, SBPI and SBPB—as good candidates for BC SSR.

DATA AVAILABILITY STATEMENT

The original contributions presented in the study are included in the article/**Supplementary Material**; further inquiries can be directed to the corresponding author.

AUTHOR CONTRIBUTIONS

BB and NW conceptualized the project. NW performed the DSC measurements. NW, KPKA, and KS conducted the rheological material characterization. NW designed and fabricated the setup and performed the direct barocaloric temperature change measurements. NW collected and analyzed all the data with guidance from BB and GS. NW and BB wrote the manuscript with input from all authors. BB, KK, and GS supervised and guided the project.

FUNDING

The material is based upon work supported by the NASA Kentucky under the NASA award number 80NSSC20M0047.

ACKNOWLEDGMENTS

We would like to thank Dr. Ian McKinley (NASA JPL, United States) for his guidance and support throughout this project. We would also like to thank Dr. Erik Usuda (CNPEM, Brazil) for advising us on the design and operation of the quasi-adiabatic temperature measurement setup.

SUPPLEMENTARY MATERIAL

The Supplementary Material for this article can be found online at: https://www.frontiersin.org/articles/10.3389/fenrg.2022.887006/full#supplementary-material

REFERENCES

Aprea, C., Greco, A., Maiorino, A., and Masselli, C. (2019a). Enhancing the Heat Transfer in an Active Barocaloric Cooling System Using Ethylene-Glycol Based Nanofluids as Secondary Medium. *Energies* 12, 2902. doi:10.3390/en12152902

Aprea, C., Greco, A., Maiorino, A., and Masselli, C. (2018a). Solid-State Refrigeration: A Comparison of the Energy Performances of Caloric Materials Operating in an Active Caloric Regenerator. *Energy* 165, 439–455. doi:10.1016/j.energy.2018.09.114

Aprea, C., Greco, A., Maiorino, A., and Masselli, C. (2018b). The Environmental Impact of Solid-State Materials Working in an Active Caloric Refrigerator Compared to a Vapor Compression Cooler. *IJHT* 36, 1155–1162. doi:10.18280/ijht.360401

Aprea, C., Greco, A., Maiorino, A., and Masselli, C. (2020). The Use of Barocaloric Effect for Energy Saving in a Domestic Refrigerator with Ethylene-Glycol Based Nanofluids: A Numerical Analysis and a Comparison with a Vapor Compression Cooler. *Energy* 190, 116404. doi:10.1016/j.energy.2019.116404

Aprea, G., Greco, M., Maiorino, A., and Masselli, C. (2019b). Is Barocaloric an Eco-Friendly Technology? A TEWI Comparison with Vapor Compression Under Different Operation Modes. *Climate* 7, 115. doi:10.3390/cli7090115

Aznar, A., Lloveras, P., Barrio, M., Negrier, P., Planes, A., Mañosa, L., et al. (2020). Reversible and Irreversible Colossal Barocaloric Effects in Plastic Crystals. *J. Mat. Chem. A* 8, 639–647. doi:10.1039/C9TA10947A

Bocca, J. R., Favaro, S. L., Alves, C. S., Carvalho, A. M. G., Barbosa, J. R., Santos, A. D., et al. (2021). Giant Barocaloric Effect in Commercial Polyurethane. *Polym. Test.* 100, 107251. doi:10.1016/j.polymertesting.2021.107251

Boldrin, D. (2021). Fantastic Barocalorics and Where to Find Them. *Appl. Phys. Lett.* 118, 170502. doi:10.1063/5.0046416

Bom, N. M., Imamura, W., Usuda, E. O., Paixão, L. S., and Carvalho, A. M. G. (2018). Giant Barocaloric Effects in Natural Rubber: A Relevant Step Toward Solid-State Cooling. *ACS Macro Lett.* 7, 31–36. doi:10.1021/acsmacrolett.7b00744

Bom, N. M., Usuda, É. O., da Silva Gigliotti, M., de Aguiar, D. J. M., Imamura, W., Paixão, L. S., et al. (2020). Waste Tire Rubber-Based Refrigerants for Solid-State Cooling Devices. *Chin. J. Polym. Sci.* 38, 769–775. doi:10.1007/s10118-020-2385-y

Brogly, M., Nardin, M., and Schultz, J. (1998). Effect of Vinylacetate Content on Crystallinity and Second- Order Transitions in Ethylene–Vinylacetate

Copolymers. *Appl. Polym. Sci.* 64, 1903–1912. doi:10.1002/(SICI)1097-4628(19970606)64:10<1903::AID-APP4>3.0.CO;2-M

Carvalho, A. M. G., Imamura, W., Usuda, E. O., and Bom, N. M. (2018). Giant Room-Temperature Barocaloric Effects in PDMS Rubber at Low Pressures. *Eur. Polym. J.* 99, 212–221. doi:10.1016/j.eurpolymj.2017.12.007

de Paula, C. H., Duarte, W. M., Rocha, T. T. M., de Oliveira, R. N., Mendes, R. d. P., and Maia, A. A. T. (2020). Thermo-Economic and Environmental Analysis of a Small Capacity Vapor Compression Refrigeration System Using R290, R1234yf, and R600a. *Int. J. Refrig.* 118, 250–260. doi:10.1016/j.ijrefrig.2020.07.003

dos Santos, W. N., Iguchi, C. Y., and Gregorio, R. (2008). Thermal Properties of Poly(Vinilidene Fluoride) in the Temperature Range from 25 to 210 °C. *Polym. Test.* 27, 204–208. doi:10.1016/j.polymertesting.2007.10.005

Fazli, A., and Rodrigue, D. (2020). Waste Rubber Recycling: A Review on the Evolution and Properties of Thermoplastic Elastomers. *Materials* 13, 782. doi:10.3390/ma13030782

Garcia-Ben, J., Delgado-Ferreiro, I., Salgado-Beceiro, J., and Bermudez-Garcia, J. M. (2021). Simple and Low-Cost Footstep Energy-Recover Barocaloric Heating and Cooling Device. *Materials* 14, 5947. doi:10.3390/ma14205947

Greco, A., Aprea, C., Maiorino, A., and Masselli, C. (2019). A Review of the State of the Art of Solid-State Caloric Cooling Processes at Room-Temperature Before 2019. *Int. J. Refrig.* 106, 66–88. doi:10.1016/j.ijrefrig.2019.06.034

Gschwandl, M., Kerschbaumer, R. C., Schrittesser, B., Fuchs, P. F., Stieger, S., and Meinhart, L. (2019). *Thermal Conductivity Measurement of Industrial Rubber Compounds Using Laser Flash Analysis: Applicability, Comparison and Evaluation Presented at the Materials Characterization Using X-Rays and Related Techniques*. Malaysia: Kelantan, 030041. doi:10.1063/1.5088299

Heckele, M., and Schomburg, W. K. (2004). Review on Micro Molding of Thermoplastic Polymers. *J. Micromech. Microeng.* 14, R1–R14. doi:10.1088/0960-1317/14/3/R01

Holden, G. (1987). "Thermoplastic Elastomers," in *Rubber Technology* (Boston, MA: Springer), 465–481. doi:10.1007/978-1-4615-7823-9_16

Janssen, S., Schwahn, D., Springer, T., and Mortensen, K. (1995). Coil and Melt Compressibility of Polymer Blends Studied by SANS and pVT Experiments. *Macromolecules* 28, 2555–2560. doi:10.1021/ma00111a059

Kashi, S., Varley, R., De Souza, M., Al-Assafi, S., Di Pietro, A., de Lavigne, C., et al. (2018). Mechanical, Thermal, and Morphological Behavior of Silicone Rubber During Accelerated Aging. *Polymer-Plastics Technol. Eng.* 57, 1687–1696. doi:10.1080/03602559.2017.1419487

Kıroğlu, C., and Kızılcan, N. (2021). Production and Characterization of Thermoplastic Elastomer Foams Based on the Styrene-Ethylene-Butylene-Styrene (SEBS) Rubber and Thermoplastic Material. *Open Chem.* 19, 929–937. doi:10.1515/chem-2021-0084

Kitanovski, A., Plaznik, U., Tomc, U., and Poredoš, A. (2015). Present and Future Caloric Refrigeration and Heat-Pump Technologies. *Int. J. Refrig.* 57, 288–298. doi:10.1016/j.ijrefrig.2015.06.008

Li, B., Kawakita, Y., Ohira-Kawamura, S., Sugahara, T., Wang, H., Wang, J., et al. (2019). Colossal Barocaloric Effects in Plastic Crystals. *Nature* 567, 506–510. doi:10.1038/s41586-019-1042-5

Li, F. B., Li, M., Xu, X., Yang, Z. C., Xu, H., Jia, C. K., et al. (2020). Understanding Colossal Barocaloric Effects in Plastic Crystals. *Nat. Commun.* 11, 4190. doi:10.1038/s41467-020-18043-1

Lloveras, P., Aznar, A., Barrio, M., Negrier, P., Popescu, C., Planes, A., et al. (2019). Colossal Barocaloric Effects Near Room Temperature in Plastic Crystals of Neopentylglycol. *Nat. Commun.* 10, 1803. doi:10.1038/s41467-019-09730-9

Lloveras, P., and Tamarit, J. L. (2021). Advances and Obstacles in Pressure-Driven Solid-State Cooling: A Review of Barocaloric Materials. *MRS Energy & Sustain.* 236, 2. doi:10.1557/s43581-020-00002-4

Maiorino, A., Del Duca, M. G., Tušek, J., Tomc, U., Kitanovski, A., and Aprea, C. (2019). Evaluating Magnetocaloric Effect in Magnetocaloric Materials: A Novel Approach Based on Indirect Measurements Using Artificial Neural Networks. *Energies* 12, 1871. doi:10.3390/en12101871

Mañosa, L., González-Alonso, D., Planes, A., Bonnot, E., Barrio, M., Tamarit, J.-L., et al. (2010). Giant Solid-State Barocaloric Effect in the Ni--Mn--In magnetic shape-memory alloy. *Nat. Mater.* 9, 4.

Miliante, C. M., Christmann, A. M., Usuda, E. O., Imamura, W., Paixão, L. S., Carvalho, A. M. G., et al. (2020). Unveiling the Origin of the Giant Barocaloric Effect in Natural Rubber. *Macromolecules* 53, 2606–2615. doi:10.1021/acs.macromol.0c00051

Min, J., Sagotra, A. K., and Cazorla, C. (2020). Large Barocaloric Effects in Thermoelectric Superionic Materials. *Phys. Rev. Mater.* 4, 015403. doi:10.1103/PhysRevMaterials.4.015403

Mirizzi, L., Carnevale, M., D'Arienzo, M., Milanese, C., Di Credico, B., Mostoni, S., et al. (2021). Tailoring the Thermal Conductivity of Rubber Nanocomposites by Inorganic Systems: Opportunities and Challenges for Their Application in Tires Formulation. *Molecules* 26, 3555. doi:10.3390/molecules26123555

Moya, X., and Mathur, N. D. (2020). Caloric Materials for Cooling and Heating. *Science* 370, 797–803. doi:10.1126/science.abb0973

Patel, S., Chauhan, A., Vaish, R., and Thomas, P. (2016). Elastocaloric and Barocaloric Effects in Polyvinylidene Di-Fluoride-Based Polymers. *Appl. Phys. Lett.* 108, 072903. doi:10.1063/1.4942000

Pottiger, M. T., Coburn, J. C., and Edman, J. R. (1994). The Effect of Orientation on Thermal Expansion Behavior in Polyimide Films. *J. Polym. Sci. B Polym. Phys.* 32, 825–837. doi:10.1002/polb.1994.090320506

Qian, S., Geng, Y., Wang, Y., Ling, J., Hwang, Y., Radermacher, R., et al. (2016). A Review of Elastocaloric Cooling: Materials, Cycles and System Integrations. *Int. J. Refrig.* 64, 1–19. doi:10.1016/j.ijrefrig.2015.12.001

Raasch, J., Ivey, M., Aldrich, D., Nobes, D. S., and Ayranci, C. (2015). Characterization of Polyurethane Shape Memory Polymer Processed by Material Extrusion Additive Manufacturing. *Addit. Manuf.* 8, 132–141. doi:10.1016/j.addma.2015.09.004

Roth, B., Wildner, W., and Drummer, D. (2020). Dynamic Compression Induced Solidification. *Polymers* 12, 488. doi:10.3390/polym12020488

Schmidt, M., Schütze, A., and Seelecke, S. (2016). Elastocaloric Cooling Processes: The Influence of Material Strain and Strain Rate on Efficiency and Temperature Span. *Apl. Mater.* 4, 064107. doi:10.1063/1.4953433

US Energy Information Administration (2021). *EIA Independent Statistics and Analysis*. Washington, DC: Total Energy.

Usuda, E. O., Imamura, W., Bom, N. M., Paixão, L. S., and Carvalho, A. M. G. (2019). Giant Reversible Barocaloric Effects in Nitrile Butadiene Rubber Around Room Temperature. *ACS Appl. Polym. Mat.* 1, 1991–1997. doi:10.1021/acsapm.9b00235

Wang, J., Hopmann, C., Schmitz, M., Hohlweck, T., and Wipperfürth, J. (2019). Modeling of pvT Behavior of Semi-Crystalline Polymer Based on the Two-Domain Tait Equation of State for Injection Molding. *Mater. Des.* 183, 108149. doi:10.1016/j.matdes.2019.108149

Wang, K., and Deng, Q. (2019). The Thermal and Mechanical Properties of Poly(Ethylene-co-Vinyl Acetate) Random Copolymers (PEVA) and Its Covalently Crosslinked Analogues (cPEVA). *Polymers* 11, 1055. doi:10.3390/polym11061055

Xu, S., Liu, J., and Wang, X. (2020). Thermal Conductivity Enhancement of Polymers via Structure Tailoring. *J. Enh Heat. Transf.* 27, 463–489. doi:10.1615/JEnhHeatTransf.2020034592

Conflict of Interest: The authors declare that the research was conducted in the absence of any commercial or financial relationships that could be construed as a potential conflict of interest.

Publisher's Note: All claims expressed in this article are solely those of the authors and do not necessarily represent those of their affiliated organizations, or those of the publisher, the editors, and the reviewers. Any product that may be evaluated in this article, or claim that may be made by its manufacturer, is not guaranteed or endorsed by the publisher.